A Simple Approach for Deriving the Symbol Error Rate of Non-Rectangular 2^{2k+1} M-Ary AMPM Modulation

Patricio Latini, Director Sales Engineering, ARRIS
Ayham Al-Banna, Sr. Staff Systems Architecture, ARRIS

Contents

Introduction

One way to achieve high data rates over band-limited channels is to increase the number of bits per symbol using optimal signal constellations designed to provide efficient performance. Nowadays, Quadrature Amplitude Modulation (QAM) is one of the most common modulation schemes used in communications systems. In particular, square QAM constellations [1] that contain even number of bits, $2k$, are widely used in many applications. Such systems have M symbols ($M=2^{2k}$), where the symbols are arranged to produce a square signal constellation.

Recently, the desire to reduce transmission errors in communications systems motivated burst receivers to support techniques like Trellis Coded Modulations (TCM) [1] in order to gain higher decoding granularity and therefore recover symbols more accurately. Since TCM mainly uses double number of symbols when compared to a standard QAM signal constellation that does not employ TCM, the need for QAM constellations with odd number of bits ($M=2^{2k+1}$) has elevated lately.

Odd-bit QAM constellations are currently used in many applications like DOCSIS and HDSL [2] [3] [4]. However, some of these applications use odd-bit QAM constellations that are not arranged in rectangular fashion. In particular, these QAM constellations are arranged such that they are a special case of Amplitude-Modulated Phase-Modulated (AMPM) signal constellations, which are designed to provide better efficiency in nonlinear distortion communication channels [5] [6]. AMPM modulation is also referred to as Carrierless Amplitude and Phase (CAP)-QAM modulation [4] [7].

Most of the previous research work has focused on rectangular even-bit QAM constellations, where a closed-form expression for the exact probability of symbol error in the presence of AWGN has already been analyzed and established [1] [8] [9] [10]. Researchers also studied odd-bit rectangular QAM constellations and developed expressions for the exact probability of symbol error after it was upper-bounded by the probability of symbol error of even-bit rectangular QAM constellations. In fact, various ways were developed, including simple geometrical procedures, to obtain a closed-form expression for the exact probability of symbol error in the presence of AWGN. Specifically, the authors in [11] proposed a geometrical approach to derive a closed-form expression for the probability of symbol error for the special case 8-symbol rectangular QAM system in the presence of AWGN. While simple geometrical approaches were used to analyze even-bit and some odd-bit rectangular QAM systems, no equivalent work has been done for the more complicated odd-bit AMPM systems, where the signal constellation is not rectangular. This paper proposes a simple

geometrical procedure to derive an expression for the exact probability of symbol error for an *M-ary* AMPM system in the presence of AWGN.

While other researchers recently developed an expression for the exact probability of symbol error for an odd-bit *M-ary* AMPM system in the presence of AWGN [7], their method was based on Craig's approach [12], which requires evaluating complicated integrals and results were only shown for an 8-CAP/QAM system. On the other hand, our paper proposes utilizing the simple familiar geometrical approach, which is used in analyzing even-bit QAM constellations, to obtain the expression for the exact probability of symbol error as well as bit error of an odd-bit *M-ary* AMPM system in the presence of AWGN. Additionally, the derived expression in this paper is verified using MATLAB-based computer simulation for an odd-bit *M-ary* ($M=2^{2k+1}$) AMPM system. The results for different modulation orders are also contrasted against the upper-bound limits for the probability of symbol error of such a system.

This paper shows that geometrical approaches can be used to evaluate the probability of symbol error in signal constellations, where the shape of decision regions is irregular and more complicated than just a square or rectangle. This geometrical approach is based on the simple and familiar concept of calculating the error probability for two-symbol Pulse Amplitude Modulated (PAM) system using the Maximum Likelihood Ratio (MLR) [1] [8] as the basis for decision.

This paper is organized as follows. Section II provides a brief overview of odd-bit *M-ary* signal constellations for which the expression of symbol error probability is derived. The derivation of the exact expression for the probability of symbol error as well as bit error using the geometrical approach is detailed in section III. Section IV compares the derived expression with previous work, simulation results, and upper-bounded system limits. Finally, the paper is concluded in Section V.

2^{2k+1} *M*-Ary AMPM Systems

Non-rectangular 2^{2k+1} *M-ary* AMPM signal constellations can be represented as two offset-overlapped 2^{2k} rectangular constellations. For example, Figure 1 shows an 8-ary AMPM system, where its constellation is broken into two rectangular constellations. Generally, the construction of each rectangular constellation is based on two orthonormal basis functions given by

$$\varphi_1(t) = \sqrt{\frac{2}{\varepsilon_g}}\mathbf{g}(t)\cos(2\pi f_c t)$$

(1)

$$\varphi_2(t) = -\sqrt{\frac{2}{\varepsilon_g}}g(t)\sin(2\pi f_c t)$$

(2)

the energy of the pulse $g(t)$. f_c is the center frequency of the modulated signal. The symbols in each constellation can then be represented via the orthonormal functions as

$$s_{ni} = A_{mi}\varphi_1 + B_{mi}\varphi_2\,, \qquad n = 1, \ldots \frac{M}{2}, i = 1,2$$

(3)

where s_{ni} is the n^{th} symbol in the i^{th} constellation. The symbols s_{ni} is composed of the combination of two levels A_{mi} and B_{mi}, in the φ_1 and φ_2 directions, respectively. The above representation of the symbol s_{ni} can be expressed as a space vector given by

$$s_{ni} = [A_{mi} \quad B_{mi}\,] = \left[\sqrt{\frac{\varepsilon_g}{2}}\cdot a_{mi} \quad \sqrt{\frac{\varepsilon_g}{2}}\cdot b_{mi}\right]$$

(4)

where a_{mi} is the m^{th} level in the φ_1 direction for the i^{th} constellation and, similarly, b_{mi} is the m^{th} level in the φ_2 direction for the i^{th} constellation. The levels a_{mi} and b_{mi} are expressed as

$$a_{mi} = \left(4m - 1 - 2\sqrt{\frac{M}{2}}\right)d\;; \quad 1 \le m \le \sqrt{\frac{M}{2}}, \qquad i = 1,2$$

(5)

$$b_{mi} = \left(4m - 1 - 2\sqrt{\frac{M}{2}}\right)d \;;\quad 1 \le m \le \sqrt{\frac{M}{2}}, \qquad i = 1,2$$

(6)

where d is the distance between two consecutive a_{mi} or b_{mi} levels and $M = 2^{2k+1}$ is the total number of symbols in the M-ary AMPM system. Observe that the total number of symbols in the above 2-constellation system is .

$$2\sqrt{\frac{M}{2}}^{2} = M$$

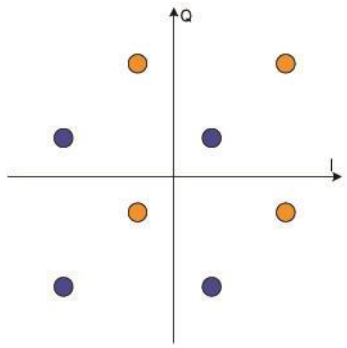

Figure 1:. Constellation of an 8-ary AMPM system is broken into two rectangular constellations

Calculating the average symbol energy of all symbols in the *M-ary* AMPM system ε_s, consists of averaging the energy of all the equally likely symbols in both constellations as 5

$$\varepsilon_s = \frac{1}{M}\sum_{\substack{n=1\ldots\frac{M}{2}\\ i=1,2}} \varepsilon_{ni} = \frac{1}{M}\sum_{\substack{n=1\ldots\frac{M}{2}\\ i=1,2}} |s_{ni}|^2$$

(7)

where ε_{ni} is the energy of the symbol s_{ni}. Expressing ε_s as the average energy of all symbols in *both constellations*, (7) can be rewritten as

$$\varepsilon_{av} = \frac{1}{M}\left[2 \cdot \sum_{m_1=1}^{\sqrt{\frac{M}{2}}}\sum_{m_2=1}^{\sqrt{\frac{M}{2}}}\left\{\left(\sqrt{\frac{\varepsilon_g}{2}}\left(4m_1 - 1 - 2\sqrt{\frac{M}{2}}\right)d\right)^2 + \left(\sqrt{\frac{\varepsilon_g}{2}}\left(4m_2 - 1 - 2\sqrt{\frac{M}{2}}\right)d\right)^2\right\}\right]$$

(8)

From (8), it can be shown that the average symbol energy in 2^{2k+1} *M*-ary AMPM system is given be

$$\varepsilon_s = \frac{\varepsilon_g}{3} d^2(2M-1) \quad (9)$$

The detector of the 2^{2k+1} *M*-ary AMPM system consists of two correlators that use φ_1 and φ_2 as reference signals. After integration over the symbol duration, the output of both correlators form coordinates of the received symbol. The process of symbols decoding depends on the MLR concept [8], where the ideal symbol closest to the received symbol (i.e., minimum Euclidean distance) is selected to be the output of the symbol detector. Since all symbols are equally likely, the decision regions represent the half-point traces between ideal symbols as shown in Figure 2 and 3. Observe that the constellations in Figure 2 and Figure 3 contain irregular-shape decision regions, which are more complicated than the familiar rectangular decision regions found in rectangular QAM systems.

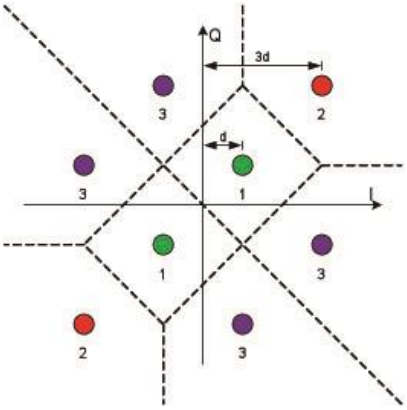

Figure 2: Different decision region types compose the constellation of an 8-ary AMPM system

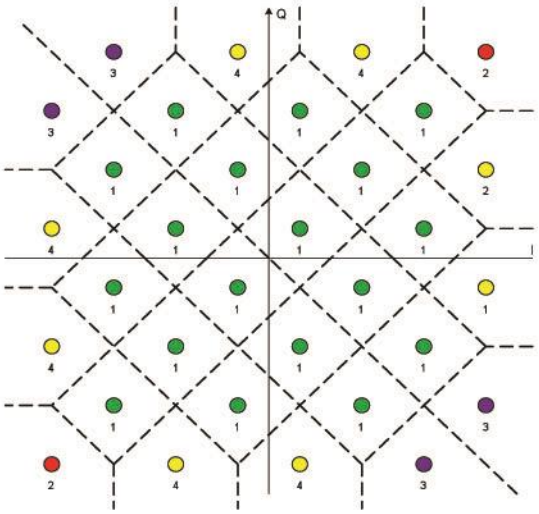

Figure 3: Different decision region types composes the constellation of a 32-ary AMPM system (General case of 4 decision region types)

Derivation of the Error Performance Expressions

In this section, we utilize geometrical approach to develop closed-form expressions for the Symbol Error Probability (SEP) and Bit Error Probability (BEP) of 2^{2k+1} M-ary AMPM system in the presence of AWGN.

Observe from Figure 2 and 3 that the constellation of an M-ary AMPM system contains four different types of decision regions denoted by Type 1, Type 2, Type 3, and Type 4 on Figure 2 and 3. The number of constellation points that belong to those regions are denoted by N_1, N_2, N_3, and N_4, respectively. They are given in Table 1.

When applying the MLR concept (shortest Euclidean distance decision rule) to decide which symbol has been transmitted, correct symbol detection occurs if the noise is small enough to keep the received symbol within the decision region of the transmitted symbol. Since the constellations under study contain four different decision regions types, the probability of correctly decoding a particular symbol will depend on the shape of the decision region of the transmitted symbol.

Decision Region	Number of constellation points
Type 1	$N_1 = 2\left(\sqrt{\frac{M}{2}} - 1\right)^2$
Type 2	$N_2 = 2$
Type 3	$N_3 = 4$
Type 4	$N_4 = \left(\sqrt{\frac{M}{2}} - 2\right)4$
Total	$N_1+N_2+N_3+N_4 = M$

Table 1: Number of constellation points in different decision regions table type styles

Therefore, the process of calculating the probability of decoding symbols correctly, P_c, involves calculating the probability of correct symbol decoding in every decision region type, which can be expressed as

$$P_c = \sum_{i=1}^{M} P_c(C|s_i)P(s_i) \quad (10)$$

where s_i is the i^{th} symbol in the M-ary AMPM constellation, $P(s_i)$ is the probability of the symbol s_i, and $P_c(C|s_i)$ is the probability of correct decoding given s_i was transmitted. When all symbols are equally likely, the probability of correct symbol decoding can be represented as

$$P_c = \frac{1}{M}\sum_{i=1}^{M} P_c(C|s_i) \quad (11)$$

Observe that the $P_c(C|s_i)$ term is a function of the transmitted symbol and therefore depends on the decision region that corresponds to that symbol. Since all symbols that correspond to each decision region are equally likely and there are only four different decision regions, the probability of correct symbol decoding, P_c, in (11) can be rewritten as

$$P_c = \frac{1}{M}\left[N_1 \cdot P_{c1} + N_2 \cdot P_{c2} + N_3 \cdot P_{c3} + N_4 \cdot P_{c4}\right] \quad (12)$$

where P_{c1}, P_{c2}, P_{c3}, P_{c4} and are the probability of correct symbol decoding given that the transmitted symbol corresponds to decision region Type 1, Type 2, Type 3, and Type 4, respectively.

The derivation starts by evaluating the probability of correct symbol decoding given that the transmitted symbol belongs to decision region Type 1 shown in Figure 4. Using the familiar MLR concept after rotating the decision region by 45°, P_{c1} can be expressed as [1] [8]

$$P_{c1} = P\left(|n_a| < \sqrt{2}d\sqrt{\frac{\varepsilon_g}{2}}, |n_b| < \sqrt{2}d\sqrt{\frac{\varepsilon_g}{2}}\right) \quad (13)$$

where n_a and n_b are the zero-mean noise components in the φ_1 and φ_2 directions, respectively, with variance of $N_o/2$, where $N_o/2$ represents the two-sided AWGN power spectral density level. It can be shown that (13) can be rewritten as [8]

$$P_{c1} = \left(1 - 2P\left(|n_a| > \sqrt{2}d\sqrt{\frac{\varepsilon_g}{2}}\right)\right)\left(1 - 2P\left(|n_b| > \sqrt{2}d\sqrt{\frac{\varepsilon_g}{2}}\right)\right)$$

$$= \left(1 - 2Q\left(\sqrt{2}\sqrt{d^2\frac{\varepsilon_g}{N_0}}\right)\right)\left(1 - 2Q\left(\sqrt{2}\sqrt{d^2\frac{\varepsilon_g}{N_0}}\right)\right)$$

$$P_{c1} = 1 - 4Q\left(\sqrt{2}\sqrt{d^2\frac{\varepsilon_g}{N_0}}\right) + 4Q^2\left(\sqrt{2}\sqrt{d^2\frac{\varepsilon_g}{N_0}}\right) \quad (14)$$

where $Q(\cdot)$ is the familiar often-tabulated function, which is the tail probability of the standard normal distribution [1].

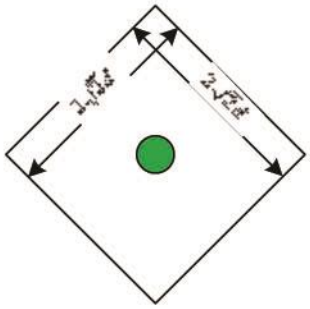

Figure 4: Decision region Type 1 in an M-ary AMPM system

Next, P_{c2}, which represents the probability of correct symbol decoding given that the transmitted symbol corresponds to the more-complicated decision region Type 2, is evaluated using geometrical approaches similar to those developed in [11]. The decision region Type 2 represents the shaded area in in Figure 5, where P_{c2} is equal to the area R_2' minus the area R_2'', where both areas are evaluated under the noise Gaussian distribution curve. That is, P_{c2} can be represented as

$$P_{c2} = P_c(C|s_2) = P_c(R_2|s_2) = P_c(R_2'|s_2) - P_c(R_2''|s_2)$$

$$P_c(R_2|s_2) = P_{R_2'} - P_{R_2''}$$

(15)

where s_2 implies that the transmitted symbol corresponds to decision region Type 2. The probability of correct decision occurring in R_2' (i.e., area of R_2'), is easily calculated using the MLR principle described above and is given by

$$P_{R_2'} = P_c(R_2'|s_2) = \left(1 - Q\left(2\sqrt{d^2\frac{\varepsilon_g}{N_0}}\right)\right)\left(1 - Q\left(2\sqrt{d^2\frac{\varepsilon_g}{N_0}}\right)\right)$$

$$P_{R_2'} = 1 - 2Q\left(2\sqrt{d^2\frac{\varepsilon_g}{N_0}}\right) + Q^2\left(2\sqrt{d^2\frac{\varepsilon_g}{N_0}}\right)$$

(16)

In order to find P_{c2}, the area R_2'' still needs to be calculated. R_2'' can be geometrically found by taking one-quarter the difference of square areas *ABCD* and *WXYZ* shown in Figure 6, which can be expressed as

$$P_{R_2''} = P_c(R_2''|s_2) = P_c(WBX|s_2) = P_{WBX}$$

$$= \frac{1}{4}(P_{ABCD} - P_{WXYZ})$$

(17)

where P_{WBX}, P_{ABCD}, and P_{WXYZ} are the areas of the *WBX* triangle, *ABCD* rectangle, and *WXYZ* rectangle, respectively, evaluated under the noise Gaussian distribution curve. P_{ABCD} can be easily found to be

$$P_{ABCD} = P_c(ABCD|s_2)$$

$$P_c(ABCD|s_2) = \left(1 - 2Q\left(2\sqrt{d^2\frac{\varepsilon_g}{N_0}}\right)\right)\left(1 - 2Q\left(2\sqrt{d^2\frac{\varepsilon_g}{N_0}}\right)\right)$$

$$P_c(ABCD|s_2) = \left(1 - 2Q\left(2\sqrt{d^2\frac{\varepsilon_g}{N_0}}\right)\right)^2$$

(18)

P_{WXYZ} can be expressed as

$$P_{WXYZ} = P_c(WXYZ|s_2)$$

$$P_c(WXYZ|s_2) = \left(1 - 2Q\left(\sqrt{2}\sqrt{d^2\frac{\varepsilon_g}{N_0}}\right)\right)^2$$

(19)

Therefore, from (17), (18), and (19), can be expressed as

$$P_{R_2''=P_{WBX}} = -Q\left(2\sqrt{d^2\frac{\varepsilon_g}{N_0}}\right) + Q^2\left(2\sqrt{d^2\frac{\varepsilon_g}{N_0}}\right) + Q\left(\sqrt{2}\sqrt{d^2\frac{\varepsilon_g}{N_0}}\right)$$

$$-Q^2\left(\sqrt{2}\sqrt{d^2\frac{\varepsilon_g}{N_0}}\right)$$

(20)

Using (15), (16), and (20), the area P_{c2} can be expressed as

$$P_{c2} = 1 - Q\left(\sqrt{2}\sqrt{d^2\frac{\varepsilon_g}{N_0}}\right) + Q^2\left(\sqrt{2}\sqrt{d^2\frac{\varepsilon_g}{N_0}}\right) - Q\left(2\sqrt{d^2\frac{\varepsilon_g}{N_0}}\right)$$

(21)

Next, P_{c3}, which represents the probability of correct detection, given that the transmitted symbol corresponds to decision region Type 3, is evaluated. P_{c3}, which is equivalent to the shaded area (R_3) in Figure 7, can be obtained by subtracting the triangle area R_3'' from the triangle area R_3' and then adding the rectangular area R_3''' to the difference, which can be written as

$$P_{c3} = P_c(C|s_3) = P_c(R_3|s_3)$$

$$P_c(R_3|s_3) = P_c(R_3'|s_3) - P_c(R_3''|s_3) + P_c(R_3'''|s_3)$$

$$P_{c3} = P_{R_3'} - P_{R_3''} + P_{R_3'''}$$

(22)

where s_3 implies that the transmitted symbol corresponds to decision region Type 3. Observe that $P_{R_3'}$ (the area of R_3') can be easily expressed as

$$P_{R_3'} = P_c(R_3'|s_3) = \frac{\left(1 - Q\left(2\sqrt{d^2\frac{\varepsilon_g}{N_0}}\right)\right)\left(1 - Q\left(2\sqrt{d^2\frac{\varepsilon_g}{N_0}}\right)\right)}{2}$$

$$P_{R_3'} = P_c(R_3'|s_3) = \frac{1 - 2Q\left(2\sqrt{d^2\frac{\varepsilon_g}{N_0}}\right) + Q^2\left(2\sqrt{d^2\frac{\varepsilon_g}{N_0}}\right)}{2}$$

(23)

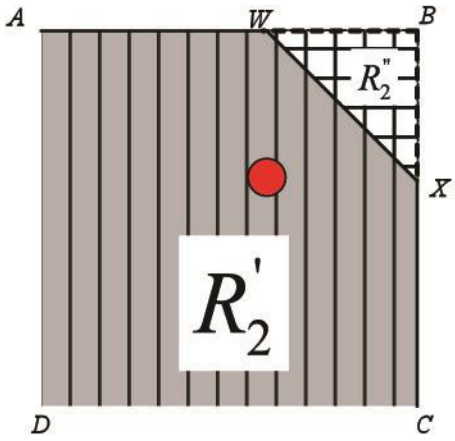

Figure 5: Detailing decision region Type 2 (R_2): R_2 is the Gray-shaded area in the figure, which equals R_2' minus R_2'', where R_2' is the open-ended vertically-hashed square area (*ABCD*) and R_2'' is the horizontally-hashed triangular area

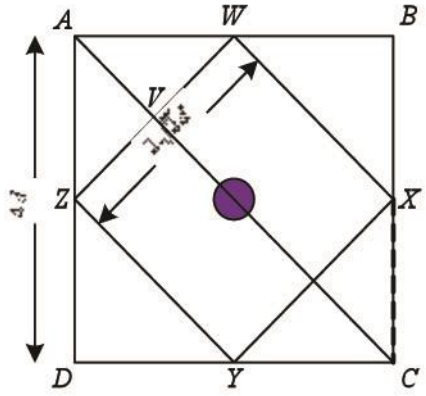

Figure 6: Calculating the area R_2'' in Figure 5. R_2'' is one-quarter the difference of square areas *ABCD* and *WXYZ*

It can be shown that the area R_3'', is half of the *WXB* triangle area calculated in (20). Therefore, the area R_3'' is given by

$$P_{R_3''} = P(R_3'|s_3) = P_c(AWV|s_2) = \frac{P_c(WBX|s_2)}{2}$$

$$P_{R_3''} = \frac{-Q\left(2\sqrt{d^2\frac{\varepsilon_g}{N_0}}\right) + Q^2\left(2\sqrt{d^2\frac{\varepsilon_g}{N_0}}\right) + Q\left(\sqrt{2}\sqrt{d^2\frac{\varepsilon_g}{N_0}}\right) - Q^2\left(\sqrt{2}\sqrt{d^2\frac{\varepsilon_g}{N_0}}\right)}{2}$$

(24)

Finally, the area R_3'' (*ZVCD*) is the half of the open-ended rectangular area (*ZWXD*) shown in Figure 7, and therefore can be easily represented by the following equation

$$P_{R_3''} = P_c(R_3''|s_2) = \frac{\left(1 - Q\left(\sqrt{2}\sqrt{d^2\frac{\varepsilon_g}{N_0}}\right)\right)\left(1 - 2Q\left(\sqrt{2}\sqrt{d^2\frac{\varepsilon_g}{N_0}}\right)\right)}{2}$$

$$P_{R_3''} = P_c(R_3''|s_2) = \frac{1 - 3Q\left(\sqrt{2}\sqrt{d^2\frac{\varepsilon_g}{N_0}}\right) + 2Q^2\left(\sqrt{2}\sqrt{d^2\frac{\varepsilon_g}{N_0}}\right)}{2}$$

(25)

Using equations (22) through (25), it can be shown that P_{c3} is given by

$$P_{c3} = 1 - \frac{1}{2}Q\left(2\sqrt{d^2\frac{\varepsilon_g}{N_0}}\right) - 2Q\left(\sqrt{2}\sqrt{d^2\frac{\varepsilon_g}{N_0}}\right)$$

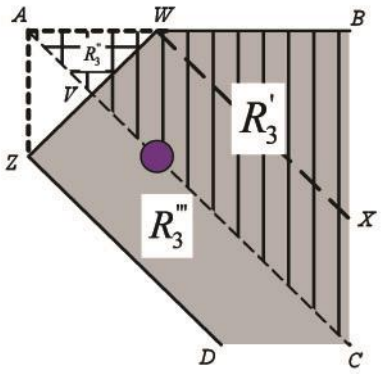

Figure7: Detailing decision region Type 3 (R_3): R_3 is the Gray-shaded area in the figure, which equals $R_3' - R_3'' + R_3'''$, where R_3' is the open-ended vertically-hashed triangular area (*ABC*), R_3'' is the horizontally-hashed triangular area (*AWV*), and R_3''' is the open-ended rectangular area (*ZVCD*).

The last step in the analysis is to evaluate P_{c4}, which represent the probability of correct symbol detection given that the transmitted symbol corresponds to decision region Type 4. P_{c4}, which represents the shaded area R_4 in Figure 8, can be obtained by subtracting the two triangles R_4' and R_4'' from the rectangular area R_4', and therefore can be written as

$$P_{c4} = P_c(C|s_4) = P_c(R_4|s_4)$$

$$(C|s_4) = P_c(R_4|s_4) = P_c(R_4'|s_4) - P_c(R_4''|s_4) - P_c(R_4'''|s_4)$$

$$P_{c4} = P_{R_4'} - P_{R_4''} - P_{R_4'''}$$

(27)

where s_4 implies that the transmitted symbol corresponds to decision region Type 4. Using the MLR principle, it can be shown that the rectangular area R_4' is given by

$$P_{R_4'} = P_c(R_4'|s_4) = \left(1 - Q\left(2\sqrt{d^2\frac{\varepsilon_g}{N_0}}\right)\right)\left(1 - 2Q\left(2\sqrt{d^2\frac{\varepsilon_g}{N_0}}\right)\right)$$

$$P_{R_4'} = 1 - 3Q\left(2\sqrt{d^2\frac{\varepsilon_g}{N_0}}\right) + 2Q^2\left(2\sqrt{d^2\frac{\varepsilon_g}{N_0}}\right)$$

(28)

The triangular areas R_4' and R_4'' are equal and can be found in a similar fashion to the area and therefore the area is given by (20), which is repeated here for convenience

$$P_{R_4'} = P(R_4'|s_4) = P_c(AWZ|s_4) = P_c(WBX|s_4) = P_{R_4''}$$

$$P_{R_4'} = P_{R_4''} = -Q\left(2\sqrt{d^2\frac{\varepsilon_g}{N_0}}\right) + Q^2\left(2\sqrt{d^2\frac{\varepsilon_g}{N_0}}\right) + Q\left(\sqrt{2}\sqrt{d^2\frac{\varepsilon_g}{N_0}}\right)$$

$$-Q^2\left(\sqrt{2}\sqrt{d^2\frac{\varepsilon_g}{N_0}}\right)$$

(29)

Using (27), (28), and (29), P_{c_4} is evaluated and found to be

$$+2Q^2\left(\sqrt{2}\sqrt{d^2\frac{\varepsilon_g}{N_0}}\right)$$

$$P_{c4} = 1 - Q\left(2\sqrt{d^2\frac{\varepsilon_g}{N_0}}\right) - 2Q\left(\sqrt{2}\sqrt{d^2\frac{\varepsilon_g}{N_0}}\right)$$

(30)

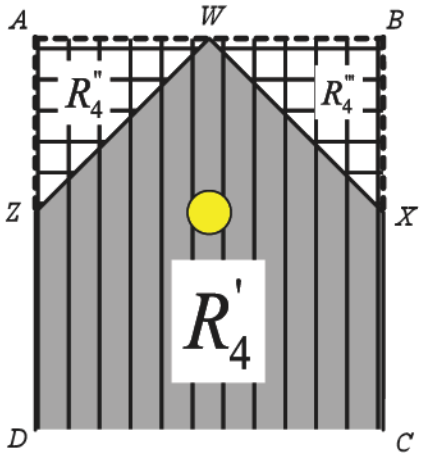

Figure 8: Detailing decision region Type 4 (R_4): R_4 is the Gray-shaded area in the figure, which equals $R_4' - R_4'' - R_4'''$, where R_4' is the open-ended vertically-hashed rectangular area (*ABCD*), R_4'' is the horizontally-hashed triangular area (*AWZ*), and R_4''' is the horizontally-hashed triangular area (*WBX*).

Finally, the total probability of correct symbol decoding, P_c, is found using (12), (14), (21), (26), and the values in Table 1. After few algebraic simplification steps, the result is given in the following expression

$$P_c = 1 + \left(-4 + 8\sqrt{\frac{1}{2M}} - \frac{2}{M}\right) Q\left(\sqrt{2}\sqrt{d^2 \frac{\varepsilon_g}{N_0}}\right)$$

$$+ \left(4 - 8\sqrt{\frac{1}{2M}}\right) Q^2\left(\sqrt{2}\sqrt{d^2 \frac{\varepsilon_g}{N_0}}\right)$$

$$+ \left(-4\sqrt{\frac{1}{2M}} + \frac{4}{M}\right) Q\left(2\sqrt{d^2 \frac{\varepsilon_g}{N_0}}\right) \quad (31)$$

The probability of symbol error for the 2^{2k+1} M-ary AMPM system in in presence of AWGN is $P_e = 1 - P_c$, which results in the following equation

$$P_e = \left(4 - 8\sqrt{\frac{1}{2M}} + \frac{2}{M}\right) Q\left(\sqrt{2}\sqrt{d^2 \frac{\varepsilon_g}{N_0}}\right)$$

$$+ \left(8\sqrt{\frac{1}{2M}} - 4\right) Q^2\left(\sqrt{2}\sqrt{d^2 \frac{\varepsilon_g}{N_0}}\right)$$

$$\left(4\sqrt{\frac{1}{2M}} - \frac{4}{M}\right) Q\left(2\sqrt{d^2 \frac{\varepsilon_g}{N_0}}\right)$$

(32)

$$P_e = \left(4 - 8\sqrt{\frac{1}{2M}} + \frac{2}{M}\right) Q\left(\sqrt{\frac{6\log_2(M)}{(2M-1)} \frac{\varepsilon_b}{N_0}}\right)$$

$$+ \left(8\sqrt{\frac{1}{2M}} - 4\right) Q^2\left(\sqrt{\frac{6\log_2(M)}{(2M-1)} \frac{\varepsilon_b}{N_0}}\right)$$

$$+ \left(4\sqrt{\frac{1}{2M}} - \frac{4}{M}\right) Q\left(\sqrt{\frac{12\log_2(M)}{(2M-1)} \frac{\varepsilon_b}{N_0}}\right)$$

(33)

which coincides with the expression provided in [7], where Craig's approach, which requires evaluating complicated integrals, was used to obtain the probability of error expression. Observe that the above expression for P_e is valid for all Odd-bit M-ary AMPM systems. Therefore, it can be used to obtain the specific probability of symbol error expressions for different odd-bit AMPM QAM systems as follows

For $M = 8$, P_e is found to be

$$P_e = \frac{9}{4}Q\left(\sqrt{\frac{6}{5}\frac{\varepsilon_b}{N_0}}\right) - 2Q^2\left(\sqrt{\frac{6}{5}\frac{\varepsilon_b}{N_0}}\right) + \frac{1}{2}Q\left(\sqrt{\frac{12}{5}\frac{\varepsilon_b}{N_0}}\right)$$

(34)

While for $M = 32$, P_e is given by

$$P_e = \frac{49}{16}Q\left(\sqrt{\frac{10}{21}\frac{\varepsilon_b}{N_0}}\right) - 3Q^2\left(\sqrt{\frac{10}{21}\frac{\varepsilon_b}{N_0}}\right) + \frac{5}{8}Q\left(\sqrt{\frac{20}{21}\frac{\varepsilon_b}{N_0}}\right)$$

(35)

and for $M = 128$, P_e is expressed as

$$P_e = \frac{225}{64}Q\left(\sqrt{\frac{14}{85}\frac{\varepsilon_b}{N_0}}\right) - \frac{7}{2}Q^2\left(\sqrt{\frac{14}{85}\frac{\varepsilon_b}{N_0}}\right) + \frac{9}{32}Q\left(\sqrt{\frac{28}{85}\frac{\varepsilon_b}{N_0}}\right)$$

(36)

Results – System Simulation and Comparison against the Upper bound limit

MATLAB®-based system simulation was performed to validate the derived expressions. Figure 9 shows complete agreement between the theoretical expressions and simulation results for different modulation orders.

The upper bound approximation limit for an odd-bit M-ary ($M=2^{2k+1}$) AMPM system is given by [reference]

$$P_e < 4\left(1 - \frac{3}{2M}\right)Q\left(\sqrt{\frac{6\log_2(M)}{2M-1}\frac{\varepsilon_b}{N_0}}\right)$$

(37)

The theoretical expressions in (34) through (36) where compared against the corresponding upper-bound limits in Figure 10. As expected, observe that the theoretical curves fall below the upper-bound limits.

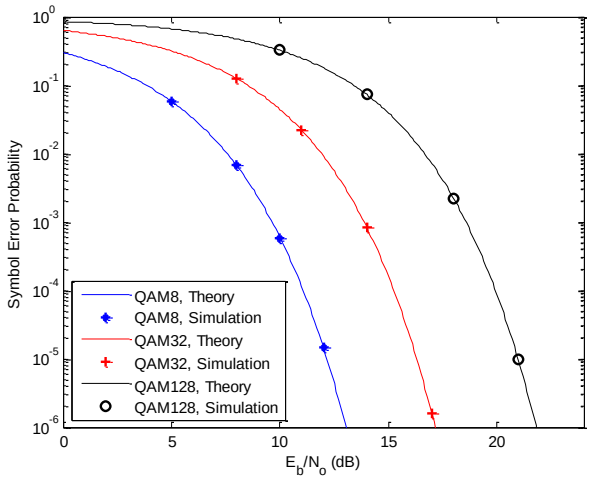

Figure 9: Exact theoretical expression results match simulations results for different modulation orders of an odd-bit *M*-ary AMPM system.

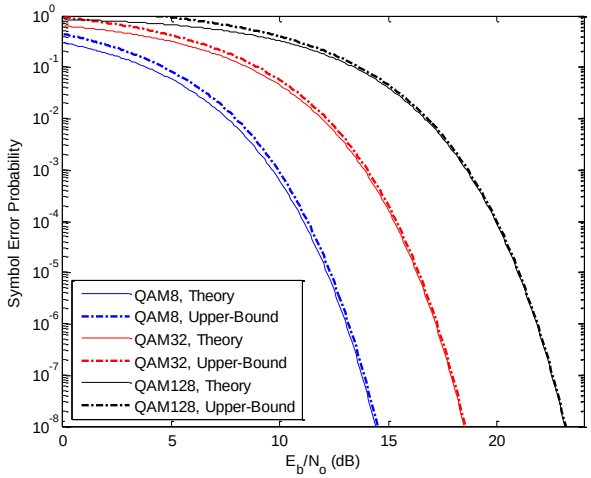

Figure 10: Exact theoretical expression results, for different modulation orders of an odd-bit *M*-ary AMPM system, sit below the known system upper-bound limits.

Conclusions

This paper proposed the use of a simple geometrical approach to develop an expression for the probability of symbol error of an odd-bit M-ary ($M=2^{2k+1}$) AMPM system in the presence of AWGN. The obtained theoretical expressions were validated using computer-based system simulations and were compared against the known upper bound limits for such systems.

References

(1) G. Proakis, *Digital Communications*, 4th Ed., McGraw-Hill Inc., 2001.

(2) Cable Television Laboratories, Inc., *Radio Frequency Interface Specification (CM-SP-RFIv2.0-C02-090422), Data-Over-Cable Service Interface Specifications (DOCSIS 2.0)*, 2009.

(3) Cable Television Laboratories, Inc., *Physical Layer Specification (CM-SP-PHYv3.0-I09-101008), Data-Over-Cable Service Interface Specifications (DOCSIS 3.0)*, 2010.

(4) J. Cioffi, T. Starr, M. Sorbara, P. J. Silverman, S. Thomas, *DSL Advances*, Prentice Hall PTR, 2002.

(5) M.G. Shayesteh, "Exact symbol and bit error probabilities of linearly modulated signals with maximum ratio combining diversity in frequency nonselective Rician and Rayleigh fading channels," *IET Commun*, Vol. 5, Iss. 1, pp. 12–26, 2011.

(6) P. Fines, A.H. Aghvami, "Performance evaluation of high level coded modulation over satellite channels," *in IEEE GLOBECOM*, pp. 417-421, 1992.

(7) M. Vaezi, J. Habibi Markani, "Exact Expression and a Simple Tight Upper Bound for the SER of Odd CAP/QAM Constellation," *in IEEE 68th Vehicular Technology Conference*, pp. 1-4, 2008.

(8) B. Sklar, *Digital communications*, 2nd Ed., Prentice Hall, 2001.

(9) M. Naeem, S. S. Shah, H. Jamal, "Performance Analysis of Odd Bit QAM Constellation," *in IEEE Symposium on Emerging Technologies*, pp. 178 – 181, 2005.

(10) H. Xu, "Symbol Error Probability for Generalized Selection Combining Reception of M-QAM," *in SAIEE Africa Research Journal*, Vol. 100, No. 3, pp. 68-71, 2009.

(11) K.H. Li, P.Y. Kam, "On the Error Performance of 8-QAM Involving a π/2-Wedge-Shaped Decision Region," *Communications and Signal Processing, 2003 and the Fourth Pacific Rim Conference on Multimedia. Proceedings of the 2003 Joint Conference of the Fourth International Conference on Information*, vol. 2, pp. 884-887, 2003.

(12) J. W. Craig, "A new, simple and exact result for calculating the probability of error for two-dimensional signal constellations," in *IEEE MILCOM'91Conf. Rec.*, Boston, MA, 1991, pp. 571-575.